Earth and Planetary Science Letters 164 (2004) 1-10

EPSL Frontiers

The evolution of El Niño, past and future

Mark A. Cane

Lamont-Doherty Earth Observatory of Columbia University
Palisades, NY 10964-8000

Abstract

We review forecasts of the future of El Niño and the Southern Oscillation (ENSO), a coupled instability of the ocean-atmosphere system in the tropical Pacific with global impacts. ENSO in the modern world is briefly described, and the physics of the ENSO cycle is discussed. Particular attention is given to the Bjerknes feedback, the instability mechanism which figures prominently in ENSO past and future. Our knowledge of ENSO in the paleoclimate record has expanded rapidly within the last 5 years. The ENSO cycle is present in all relevant records, going back 130 kyr. It was systematically weaker during the early and middle Holocene, and model studies show that this results from reduced amplification of anomalies in the late summer and early fall, a consequence of the altered mean climate in response to boreal summer perihelion. Data from corals shows substantial decadal and longer variations in the strength of the ENSO cycle within the past 1000 years; it is suggested that this may be due to solar and volcanic variations in solar insolation, amplified by the Bjerknes feedback. There is some evidence that this feedback has operated in the 20th century and some model results indicate that it will hold sway in the greenhouse future, but it is very far from conclusive. The comprehensive general circulation models used for future climate projections leave us with an indeterminate picture of ENSO's future. Some predict more ENSO activity, some less, with the highly uncertain consensus forecast indicating little change.

1. Introduction

Given time, we are a very adaptable species. Humans survive, and even flourish, in climates ranging from tropical to arctic, from arid to rain forest. In common with most species, however, we are troubled by rapid changes in climate. A few years of well below average rainfall in some normally well-watered farmlands may fairly be described as "a devastating drought", although the same level of rainfall might mean a bountiful harvest in a savannah.

Within our lifetimes, the most dramatic, most energetic, and best-defined pattern of climate changes has been the global set of anomalies referred to as ENSO (El Niño and the Southern Oscillation). The very strong and very heavily reported event in 1997-98 brought El Niño worldwide notoriety. It is implicated in catastrophic flooding in coastal Peru and Ecuador, drought in the Altiplano of Peru and Bolivia, the Nordeste region of Brazil, and Indonesia, New

Guinea and Australia. Huge forest fires on Kalimantan spread a thick cloud of smoke over Southeast Asia and crippled air travel by shutting down airports in Singapore, Malaysia and Indonesia.

While there is a tendency to hold El Niño responsible for just about anything unusual that happened anywhere, the listed climate impacts are ones that investigations of events in the past century have shown to be strongly correlated with El Niño. Of course, every year there are droughts and floods somewhere. Goddard (2004) points out that, paradoxically, El Niño years may come to be the least costly. Unlike the seemingly random set of climate hazards in a typical year, those associated with El Niño are predictable a year or more ahead (Goddard et al 2001; Chen et al 2004). This could allow preparations that would mitigate the impacts of El Niño related climate anomalies. For example, given prior warning of the 1997-98 El Niño, in anticipation of heavy rains the city of Los Angeles cleared storm drains to prevent flooding. Even without good predictions of particular events, there can be adaptive advantages just in knowing the longer-term patterns. Farmers in Queensland now understand that as a consequence of the ENSO cycle, it is likely that they will make money only 3 years out of 10, and plan accordingly. In *Guns, Germs and Steel*, Jared Diamond argues that since agriculture was doomed to fail so often, aboriginal Australians were correct to remain as hunter-gatherers, a choice with the most profound cultural consequences.

All of us now anticipate a change in climate brought about by human activity. Among other things, we will have to adjust to a change in the year-to-year variations in climate. Will there be more El Niños, or more powerful El Niños? Will the impacts of the ENSO cycle change? Over the past century, the period for which we have instrumental data, there is a statistically significant association between poor monsoons in India and El Niño events. This relationship seemingly broke down in the 1990s (Kumar et al, 1999); monsoon rainfall was near normal during the powerful 1997 event. In contrast during the very strong 1877 El Niño there was severe drought in Indian leading to widespread famine. Kumar et al (1999) speculated that the change in the monsoon-ENSO relationship might be a consequence of global warming. However, the "normal" association seemingly has returned, as the moderate 2001-02 El Niño was accompanied by a weak monsoon.

So, how will El Niño change in a greenhouse world? The short answer, to be expanded upon in Sec. 4, is that the best estimate is that it will not change much at all, but we have very low confidence in this answer. We begin in Sec 2 with a brief review of salient features of ENSO observed in the modern, instrumental record. We touch on ideas about the physics of ENSO, ideas that are useful in considering how ENSO behavior can change. ENSO's past is reviewed in Sec. 3. The last few years have seen a great increase in our knowledge of ENSO in the Holocene and late Pleistocene. The changes over this time, and our ability to explain them, offer some guidance for the future.

2. ENSO in the Present

Figure 1 shows two widely used indices for ENSO over the past century and a half. The term "El Niño" was used long ago by Peruvian fisherman for the annual warming of coastal waters that occurs around Christmas time. Scientists now reserve the term for a warming of the eastern equatorial Pacific, though there is no widely accepted definition of how much of a warming over exactly what region it takes to qualify as an "El Niño". NINO3, which refers to the sea surface temperature (SST) anomaly in the NINO3 region (90W-150W, 5S-5N) of the eastern equatorial Pacific, is a commonly used index of El Niño. The "Southern Oscillation" is a see-sawing of atmospheric mass, and hence of sea level pressure (SLP), between the eastern and western Pacific. It is most often indexed by the Southern Oscillation Index (SOI), a normalized SLP difference between Darwin, Australia and Tahiti. In Fig. 1 we simply use SLP at Darwin, which is almost the same because the anti-correlation between Tahiti and Darwin is so high. There is a striking similarity between the two measures, one atmospheric and one oceanic, widely separated in space. Clearly, they index the same phenomenon.

The most obvious features of the records in Fig. 1 are the irregular oscillations occurring about every 4 years (2-7 years is usually taken as defining the ENSO band). Some time periods such as the late 19th or 20th centuries are marked by numerous high amplitude oscillations, while others (e.g. the 1930s) are rather quiet.

There is now a widely accepted explanation for the oscillation, built upon Jacob Bjerknes' (1969) masterpiece of physical reasoning from observational data (See Cane, 1986 for a more detailed historical account of ENSO theory). Bjerknes marked the peculiar character of the "normal" equatorial Pacific: although the equatorial oceans all receive about the same solar insolation, the Pacific is 4-10°C colder in the east than in the west (see Fig 2). The east is cold because of equatorial upwelling, the raising of the thermocline exposing colder waters, and the transport of cold water from the South Pacific. All of these are dynamical features driven by the easterly trade winds. But the winds are due, in part, to the temperature contrast in the ocean, which results in higher pressures in the east than the west. The surface air flows down this gradient. Thus the state of the tropical Pacific is maintained by a coupled positive feedback: colder temperatures in the east drive stronger easterlies which in turn drive greater upwelling, pull the thermocline up more strongly, and transport cold waters faster, making the temperatures colder still. Bjerknes, writing in the heyday of atomic energy, referred to it as a "chain reaction". We now prefer "positive feedback" or "instability".

Bjerknes went on to explain the El Niño state with the same mechanism. Suppose the east starts to warm; for example, because the thermocline is depressed. Then the east-west SST contrast is reduced so the pressure gradient and the winds weaken. The weaker winds bring weaker upwelling, a sinking thermocline, and slower transports of cold water. The positive feedback between ocean and atmosphere is operating in the opposite sense (see Fig 2). Note that this explanation locks together the eastern Pacific SST and the pressure gradient – the Southern Oscillation – into a single mode of the ocean-atmosphere system, ENSO.

Bjerknes' mechanism explains why the system has two favored states but not why it oscillates between them. That part of the story relies on the understanding of equatorial ocean dynamics that developed in the two decades after he wrote. The key variable is the depth of the thermocline, or, equivalently, the amount of warm water above the thermocline. The depth changes in this warm layer associated with ENSO are much too large to be due to exchanges of heat with the atmosphere; they are a consequence of wind driven ocean dynamics. Let us begin at the peak of a warm (El Niño) event (Fig. 3a). The thermocline is deep in the east and the SST is warm there; hence the trades are weak (the anomalies are westerly), driving Kelvin waves along the equator making the east warmer still. This is the Bjerknes feedback operating in its warm phase.

But the excess of upper ocean warm water in the east must be compensated somewhere, so the thermocline at the western side of the Pacific is anomalously shallow. The anomalies' shape and location is dictated by the special character of equatorial ocean dynamics. When the warm (deepening) packet of equatorial Kelvin waves hits the eastern coast (South America in the real Pacific) it is reflected as Rossby waves, which propagate westward. The closer they are to the equator the faster they move, so the reflection pattern is broad near the equator, narrowing as latitude increases (viz. Fig. 3). Meanwhile, the cold (shallowing) signal in the west propagates as packets of equatorial Rossby waves, moving westward at speeds 1/3 or less of the Kelvin wave speed,. In contrast to the equatorial Kelvin waves, their height extrema (minima, in this case) are off the equator. Upon reaching the western boundary they are collected in equatorward propagating boundary currents and finally reflected as equatorial Kelvin wave packets that carry this shallowing signal to the east. There it counters the deepening due to the Kelvin waves that were directly wind forced in the central Pacific. The deepening slows, then stops, then reverses; the El Niño is winding down (Figs 3b), and the process proceeds until the eastern thermocline reaches its normal depth (Fig. 3c). At this time the thermocline and temperature gradients along the equator are near normal, so the winds are also near normal. At this point, if all depended on the Bjerknes feedback, then the cycle would come to a stop. But even without any wind driving, the cold anomalies in the west (Fig. 3c) continue to propagate freely to the western boundary to be reflected eastward along the equator. A cold anomaly is now created in the east (Fig 3d) and the Bjerknes mechanism begins to create easterly anomalies (i.e. strong trades). Now the stronger trades send Kelvin waves to withdraw upper layer fluid from the east, and Rossby waves to add it to the west (Fig 3e). Thus the oscillation continues. This mechanism is referred to as the "delayed oscillator".

There are two elements in this story: the coupled Bjerknes feedback and the (linear) wave propagation, which introduces the out-of-phase element required to make an oscillator. If the coupling were strong enough, then the direct link from westerly wind anomaly to deeper eastern thermocline to warmer SST and back to increased westerly anomaly would build too quickly for the delayed, indirect shallowing signal to ever catch up. The "coupling strength" is determined by a host of physical factors. Among the most important: how strong the mean wind is, which influences how much wind stress is realized from a wind anomaly; how much atmospheric heating is generated by a given SST change, which will depend on mean atmospheric temperature and humidity; how sharp and deep the climatological thermocline is, which together determine how big a change in the temperature of upwelled water is realized from a given wind-driven change in the thermocline depth. The impact on ENSO frequency and amplitude of these and other factors have been discussed from the beginnings of ENSO modeling (e.g. Zebiak and Cane, 1987), but Federov and Philander (2000, 2001) have recently provided a far more comprehensive study.

In very simple linear analyses (Battisti and Hirst, 1989; Cane et al, 1990) the period is set by the competition between the direct and delayed signal as determined by the coupling strength. In a more realistic nonlinear model this general statement still holds, but the periods tend to stay within the 2-7 year band. There is no satisfactory theory explaining why this is so, or more generally, what sets the average period of the ENSO cycle. There is broad disagreement as to why the cycle is irregular; some attribute it to low order chaotic dynamics, some to noise –weather systems and intraseasonal oscillations -- shaking what is essentially a linear, damped system. We will return to these issues as we consider ENSO past and future.

3. ENSO in the Paleoclimate Record

There is good evidence that the ENSO cycle has been a feature of the earth's climate for at least the past 130,000 years (Tudhope et al 2001; Hughen et al, 1999). Fig. 4 shows records from fossil corals collected on the Huon Peninsula, a location in ENSO's "heartland". The oxygen isotope signal primarily reflects variations in rainfall, which has much greater range there than temperature. In any case, since greater precipitation and warmer temperatures occur together there, we can take $\delta^{18}O$ as an index of ENSO without troubling to disentangle the temperature and salinity signals. Every record shows oscillations in the 2-7 year band characteristic of ENSO. Since the records cover only a small fraction of the time since the last interglacial, so the possibility of some period without oscillations or with markedly different oscillations cannot be ruled out. However, there are enough records to be able to say that if there are such periods they cannot be common. It is interesting to note that an ENSO model (Clement et al 2001) shows ENSO stopping only twice in the past 500, 000 years: during the Younger Dryas, and about 400 kyr earlier when the orbital configuration was most similar to the Younger Dryas.

An earlier study of a laminated core from a lake in Ecuador (Rodbell et al 1999; also see Moy et al, 2002) was often interpreted as showing an absence of ENSO in the early and middle Holocene (Rodbell et al 1999; Federov and Philander, 2000, 2001). The proxy for ENSO is the clastic sediment washed into the lake during the heavy rains that occur almost exclusively during El Niño events It is consistent with the Tudhope et al (2001) record to suppose that although the ENSO cycle continues, there were few El Niño events during this period strong enough to wash material into the lake. In this view, ENSO does not start circa 5000 BP, but merely picks up strength. Because ENSO amplitudes can vary so much over a century (e.g. Fig 1), the fossil coral records are too short and too few to allow a confident statement that the early and middle Holocene were surely marked by a weakened ENSO cycle. The lake record, however, covers the whole period, and shows a systematic difference between the early-middle Holocene and the last 5000 years. The fossil coral records strongly suggest that the ENSO cycle was also weaker than at present during the glacial era, and of comparable amplitude to the modern during the last interglacial. More records are needed to establish that this description is indeed correct.

A continuing middle Holocene controversy is whether the mean state of the eastern equatorial Pacific was warmer or colder than today. On the basis of warm water mollusk shells found on the coast of Peru at latitudes where they are not present today, Sandweiss et al (1996) inferred that the mean temperatures were warmer – a persistent El Niño state. This is not consistent with other geological evidence or the proxy temperature record of Koutavas et al (2002). Moreover, if an El Niño-like state prevailed, there should have been more rain at the lake sites in Ecuador. Clement et al (2000) suggest that the mollusks survive because they were not subjected to the extreme cold temperatures that occur with La Niña today since the cold (La Niña) phase of ENSO was also weaker at this time.

Why was the behavior of ENSO so different in the early and middle Holocene? Clement et al (2000) show that the cause is the difference in the earth's orbital configuration at that time. Using the ENSO model of Zebiak and Cane (1987) they impose the perturbation heating due to orbital changes to an otherwise modern state. The model simulation has a weaker ENSO cycle during the early and middle Holocene. The average period between events is not greatly different, but strong events are rare. In both the model and real versions of the modern climate, ENSO events amplify through a "growing season" that runs through the boreal summer and into the autumn, after which growth ceases and anomalies begin to decay. (Thus El Niño and La Niña events peak around the end of the calendar year, when the rate of change is zero.) The growth is a consequence of the Bjerknes feedback; there is a positive feedback for only part of the year. In the model simulations of the early Holocene the growth of anomalies ends around August, before the summer is over. This shorter growing season means that anomalies do not reach the peak values of today.

The equatorial oceans received about the same annual solar radiation but its seasonal distribution is quite different. Northern hemisphere insolation was stronger in the late summer and fall, so the Intertropical Convergence Zone (ITCZ), which tends to lie over the warmest water, was held more firmly in place in the higher tropical latitudes. A key link in the Bjerknes feedback is from SST to enhanced heating to changes in the winds, but the heating is associated with low level convergence, and if the convergence cannot be moved on to the equator the link is broken and the ENSO anomalies do not grow. This analysis is based on a model of intermediate complexity, one that omits mechanisms that might alter the outcome, such as the advection of subsurface temperature anomalies. However, CSM, the NCAR (National Center for Atmospheric Research) comprehensive coupled General Circulation Model (GCM) has also been shown to have a weak amplitude ENSO cycle at 9kyr BP and 6 kyr BP (Otto-Bliesner et al, 2003).

Thus orbital changes alter the mean climate and this in turn changes ENSO behavior markedly. The Tudhope et al (2001) records also suggest that ENSO was weakened by glacial conditions at times when the model, which sees only orbital changes, maintains its strength. The changes in orbital forcing and from modern to glacial are both strong perturbations. Very recent studies of ENSO over the last millennium provide examples of shifts in ENSO behavior without strong forcing. These are shifts in ENSO variance, typically associated with changes in mean temperatures in the eastern equatorial Pacific, with timescales of decades to perhaps centuries. They could be a consequence of unforced natural variability, but, as discussed below, are more likely a response to the variations in radiation forcing due to volcanic activity and changes in solar output. These forcings are not only much weaker than the orbital changes, but they have far less seasonal and latitudinal structure, so they provide more direct lessons for the greenhouse climate.

Decadal variations in ENSO are intertwined with Pacific-wide decadal variations. In the tropical Pacific the Pacific Decadal Variation (PDO) has a pattern much like ENSO but broader; it has its largest amplitude in the midlatitude North Pacific (Mantua et al 1997; Zhang et al 1997). Recent work has shown that there are decadal variations in the South Pacific, strongly expressed in the movement of the South Pacific Convergence Zone, and that these are linked to the PDO (Garreaud and Battisti, 1999; Power et al, 1999; Deser et al, 2004). Power et al

(1999), noting that "PDO" is usually taken to be centered in the North Pacific, use "Interdecadal Pacific Oscillation" (IPO) to emphasize the basin wide nature of Pacific variability. Having the signal appears in both hemispheres implicates the tropics as a likely source, and some of this work shows a direct connection in the data (see especially Deser et al, 2004). How much of the basin wide decadal variability is driven from coupled interactions in the tropical Pacific similar to ENSO, and how much is attributable to mid-latitude sources is an area of active research. The IPO (or PDO) has been shown to affect the connections between ENSO and rainfall in Australia (Power et al, 1999) and North America (Gershunov and Barnett 1998). It appears that the total SST perturbation in (at least) the tropical Pacific must be considered to capture global impacts; ENSO alone is insufficient.

It is difficult to reach firm conclusions about decadal variations from the instrumental record, since it is only long enough to provide half a dozen or so instances. The principal proxies able to resolve decadal variations are tree rings and isotopic analyses of corals. Both are at annual resolution and also resolve ENSO. The relevant tree rings are primarily proxies for precipitation in places where the influence of ENSO and the IPO are strong. They are thus indirect proxies for ENSO, subject to other large-scale climate influences as well as the usual local and biological effects. This problem can be overcome by using multiple sites to extract the signal that corresponds to ENSO or the IPO; see Mann, 2002 for a broad discussion. This approach has been used by a number of investigators to construct indices of the IPO going back several centuries, primarily using tree rings, (Biondi et al 2001; D'Arrigo et al 2001; Gedalov and Smith 2001; Villalba et al 2001), but also using both tree ring and coral data (Evans et al 2001, 2000; Mann et al 2000) and corals alone (Evans et al 2002).

The corals from a given site used in these reconstructions have been a single coral head, allowing records of a few hundred years or less. Cobb et al (2003) overlapped shorter segments of fossil coral in a manner similar to the way tree ring time series have been spliced together from individual trees. The result is displayed in Figure 5. Palmyra (6°N, 162°W) is in a prime location to provide an ENSO proxy, and the correlation of Cobb et al's $\delta^{18}O$ record from modern corals with the NINO3.4 (120°W to 170°W, 5°S to 5°N) SST is –0.84 in the ENSO band. In other words, this coral proxy series correlates as well or better as any two commonly used ENSO indices (e.g. SOI, NINO3, NINO3.4) correlate with each other. It is likely that the $\delta^{18}O$ signal primarily reflects rainfall and so correlates better with NINO3.4 than with local SST (see Evans et al 2002).

Figure 5 also displays the results of a 100 member ensemble calculated by Mann et al (2004) forcing the Zebiak-Cane model with a slightly updated version of the Crowley (2000) solar and volcanic forcing. Regardless of whether it is noise-driven or a consequence of chaos, the variability of ENSO makes it impossible that even a perfect model would agree in detail with the single realization present in the observational record. If the ENSO variability is forced, then it is possible for values averaged over a number of ENSO events to agree. Indeed, Figure 5 shows, for both model and data, cold SSTs in the mean in the late 12th – early 13th centuries, moderate SSTs in the 14th- early 15th centuries, and warm SSTs in the late 17th century. In all three cases the means of the observations and the model ensemble are consistent within the ensemble sampling distribution (dotted red lines on Fig 5). Moreover, the late 17th century warmth and the 12-13th century cold are well separated within the distribution of states from the model ensemble runs: one would expect the later period to be warmer than the earlier one in roughly 7 out of every 8 realizations. Applying these statistics to reality, we would expect nature's single realization to be warmer in the later period with close to a 90% probability. In both data and model there is also a systematic difference in the strength of the ENSO cycle in the two periods. There are numerous large El Niño events in the late 17th century and very few in the 12th to early 13th century period. (This difference is statistically significant at the 0.1 level for both model and data.) Thus more (less) ENSO variability goes with a colder (warmer) mean SST in the eastern equatorial Pacific.

The differences -- in the model run, at least -- are a consequence of the Bjerknes mechanism. The result is, at first, counterintuitive: the warmer tropical Pacific temperatures occur at a time of increased volcanic activity and global cooling (Crowley, 2000; Jones et al 2001) and visa versa. If there is a cooling over the entire tropics then the Pacific will change more in the west than in the east because the strong upwelling in the east holds the temperature closer to the pre-existing value. Hence the east-west temperature gradient will weaken, so the winds will slacken, so the temperature gradient will decrease further – the Bjerknes feedback, leading to a more El Niño-like state. This chain of physical reasoning is certainly correct as far as it goes, and the agreement between the data and the simulation with the simplified Zebiak-Cane model is evidence for the idea that the Bjerknes feedback holds sway in response to a change in radiation forcing. But the climate system is complex and processes not considered in this argument, such as cloud feedbacks, might be controlling.

4. ENSO in the Future

Before turning to model projections of the future, we briefly consider what can be learned from the changes since the rise of CO_2 began in earnest in the late 19th century. Trenberth and Hoar (1997), noting that greenhouse gas concentrations rose sharply in the past few decades, argued that the increase in the frequency and amplitude of ENSO events in the 1980s and 1990s was highly unusual, significantly different from the behavior in the preceding century, and thus attributable to anthropogenic causes. Rajagopalan et al (1997) used a different statistical model to formulate their null hypothesis and concluded that the behavior was not significantly different from that in the earlier part of the instrumental record (also see Wunsch, 1999). The arguments are technical and inconclusive; the reader is invited to compare the last quarter of the 20th century with the last quarter of the 19th century in Figure 1 and decide if the level of ENSO activity in the two eras is strikingly different. By some measures the 1877 El Niño was more powerful than any of the events in the 20th century. Record drought in India, as well as severe droughts in Ethiopia, China, Northeast Brazil and elsewhere, all contributed to what is fairly described as a global holocaust (Davis, 2001).

We noted that the data of Cobb et al (2003) showed cooling in the eastern equatorial Pacific at times in the past when the global climate warmed due to increased solar radiation or reduced volcanism, a result reproduced in the modeling study of Mann et al (2004) and explained by the Bjerknes feedback. However, this same relation does not seem to hold for the 20th century, when radiative forcing, global temperatures, and NINO3 SST all increase. (Crowley, 2000 found the greatest disagreement between global mean temperature and a model forced by solar, volcanic and greenhouse gas variations in the early 20th century.) Perhaps this change in behavior is due to the impact of atmospheric aerosol or perhaps there is something missed in our argument when the radiative increase is due to increased greenhouse gases. Another possibility is suggested by the result of Cane et al (1997), whose plots of temperature trends from 1900 to 1991 are updated to 2000 in Fig 6. Fig. 6 shows essentially no change in the eastern central Pacific. (Cane et al found a slight cooling, but it was not significantly different from zero in the NINO3.4 region.) However, the data in this region is quite sparse, so this conclusion is not robust. But the east-west SST gradient does become significantly stronger over the century – as would be expected from the Bjerknes feedback (Fig 6, bottom panel).

If we are to trust a model to predict ENSO in the greenhouse world, it is necessary that it reproduces the changes in prior centuries, but it may not be sufficient. In addition to simulating changes, it greatly increases our confidence if the model can simulate the defining features of the ENSO cycle with some skill. Is the mean frequency close to 4 years? Is the largest warm anomaly where it is observed in the eastern equatorial Pacific? Does the model's cold tongue extend too far to the west, into the warm pool region? Unfortunately, few of the comprehensive Coupled General Circulation Models (CGCMs) get these features right. AchutaRao and Sperber (2002) reviewed the simulations of ENSO in 17 CGCMs that were part of the Coupled Model Intercomparison Project (CMIP). Most of the model El Niños were too weak and markedly in the wrong location. Five of the models were judged to "represent well the Walker circulation anomalies, the warming and enhanced rainfall in the central/east Pacific." Some of these model ENSOs had most of their power at a higher frequency (~ 2 years) than observed, and most did not have the correct phase with respect to the annual cycle.

Collins et al. (2004) investigated the predictions from 20 CMIP CGCMs of changes in ENSO due to 1% per year increases in greenhouse gases. Figure 7 summarizes the results. The top panel shows the histogram over the 20 model results of a measure of whether the mean state becomes more El Niño-like or more La Niña-like. The most probable outcome is no large trend in either direction. The middle panel is the histogram weighted by how well the model simulates ENSO in the present climate. The measure of quality used is obviously somewhat arbitrary, but the results are not very different from the unweighted histogram and would be qualitatively the same for any sensible measure. As the bottom panel shows, the models that do the best simulations predict small changes.

The ENSO cycle depends on the seasonal cycle, as is obvious from its tendency to have a pattern of evolution locked to the calendar. Few CGCMs are capable of realistic simulations of the climatology of the real world. This problem can be "fixed" with "flux corrections", empirical terms added to push the model away from its own climatology toward the observed one. Such a fix raises questions as to whether or not the flux-corrected model will have the correct variability or the correct sensitivities to greenhouse gases. Strenuous efforts are now made to avoid flux corrections. Much of the difficulty models have with ENSO variability is a consequence of their poor tropical Pacific mean climates. Rather small changes have great consequence, as succinctly illustrated in Collins (2000). In simulations of a 4xCO_2 world, the HADCM2 model, which was flux corrected, had a stronger ENSO at a higher frequency than in a control simulation. A 4xCO_2 simulation with HADCM3, an improved version of HADCM2 (no flux correction, higher resolution, improved process parameterizations), showed no change in ENSO. The two models have different mean states in the control runs, and different changes in the $4xCO_2$ world. These differences in the mean, which are primarily due to subtle differences in the parameterization of low cloud, account for the differences in ENSO response.

Doherty and Hulme (2002) looked at the simulations from 12 CGCMs of changes in the SOI and tropical precipitation from 1900 to 2099. (Data from these 12 are available at the IPCC Data Distribution Centre; many are also in the CMIP set.) They report that changes in SOI variability are not coherent among the models, broadly consistent with Collins et al (2004). They do find an overall tendency toward a more positive SOI – a more La Niña-like state. Specifically, 6 of the simulations showed a statistically significant positive trend and 2 a statistically significant negative (El Niño-like) trend, while the remaining 4 showed no significant trends.

The positive trend is in keeping with expectations based on the Bjerknes feedback, but was surprising because two of the earliest studies of ENSO in the greenhouse with this generation of models reported a positive (more El Niño-like) trend in NINO3 (Timmermann et al, 1999; Cai and Whetton, 2000). Moreover, the models used in these studies, ECHAM4 and CSIRO, are among the ones found to have positive trends in the SOI. One possible reason for the discrepancy between the two measures of ENSO is that a trend toward more La Niña-like SSTs in the eastern Pacific is overridden by the overall global warming; it would be revealed by looking at east-west temperature gradients instead of NINO3, as is the case for the 20th century observations in Figure 6. Or, it might be that the overall pattern of the ENSO events is altered in the greenhouse world; for example, a shift to the southeast as observed in the late 20th century by Kumar et al (1999). Doherty and Hulme (2002) found pattern changes in a minority of the 12 simulations they considered, with HADCM2 and ECHAM4 showing eastward shifts.

Conclusions

Glendower: I can summon spirits from the vasty deep.
Hotspur: why, so can I, or so can any man; but will they come when you do call for them?
Henry IV, Part 1, Act 3 Scene 1

ENSO variations impact climate world wide because the changes in the heating of the tropical atmosphere they create alter the global atmospheric circulation. Changes in the mean state of the tropical Pacific would have similar impacts. Since societies and ecosystems are profoundly affected, we would like to know how ENSO and the mean state of the tropical Pacific will change in our greenhouse future. We must rely on models to make such predictions, since the past does not provide a true analogue of the new climate we are creating.. Our comprehensive coupled general circulation models are impressive achievements, now able to simulate many features of the climate with striking verisimilitude. The ENSO cycle, however, is not their forte. Present attempts to summon the ENSO of the future bring forth a motley and uncertain set of responses. The paleoclimate record shows us that ENSO behavior is quite sensitive to climatological conditions, so it stands to reason that ENSO will behave differently in the future. But we can't say how it will differ with any confidence. Indeed, the models' consensus estimate is that it won't change much at all.

There are reasons for optimism. The quality of ENSO simulations has improved dramatically in the past decade, and further progress is likely if computing power grows adequately. The paleoclimate record, almost devoid of information about ENSO only 5 years ago, is expanding rapidly and even now provides enough information to test models under conditions substantially different from modern. Thus there is hope that we can soon increase our confidence in forecasts of future variability. But for the present, the future of ENSO lies in depths of vast uncertainty, beyond our summons.

Acknowledgements. Thanks to Alexey Kaplan, Naomi Naik, Amy Clement, Sandy Tudhope and Matt Collins for valuable discussions, and to Naomi Naik and Alexey Kaplan for help with figures and Virginia DiBlasi for help with ms preparation. This work was supported by NOAA grants NA03OAR4310064 and NA03OAR4320179 and NSF grant ATM0347009.

REFERENCES

AchutaRao, K. and K.R. Sperber, 2002: Simulation of the El Niño Southern Oscillation: Results from the Coupled Model Intercomparision Project, *Climate Dynamics,* **19**, 191-209.

Battisti, D.S. and AC. Hirst, 1989: Interannual variability in a tropical atmosphere-ocean model: influence of the basic state, ocean geometry, and nonlinearity. *J. Atmos. Sci*., **46**, 1,687-1712.

Bjerknes, J., 1969: Atmospheric teleconnections from the equatorial Pacific, *Mon. Weath. Rev*., **97**, 163-172.

Biondi, F., A. Gershunov, and D.R. Cayan, 2001: North Pacific decadal climate variability since 1661, *Journal of Climate*, **14** (1), 5-10.

Cai, W. and P.H. Whetton, 2000: Evidence for a time-varying pattern of greenhouse warming in the Pacific Ocean, *Geophys. Res. Lett.*, **27**, 2577-2580

Cane, M.A., 1986: El Niño. *Annual Review of Earth and Planetary. Sci,* **14,** 43-70.

Cane, M.A., M. Münnich and S.E. Zebiak , 1990: A study of self-excited oscillations of the tropical ocean- atmosphere system. Part I: linear analysis. *J. Atmos. Sci*., **47**, 1,562-1,577.

Cane, M.A., A.C. Clement, A. Kaplan, Y. Kushnir, R. Murtugudde, D. Pozdnyakov, R. Seager and S.E. Zebiak, 1997: 20th century sea surface temperature trends. *Science*, **275**, 957-960.

Chen, D., A. Kaplan and M.A. Cane, 2004: Application of Altimeter Observations to Tropical Ocean Modeling and Climate Prediction, *Intermat. J. of Remote Sensing*, **22**, 2621-2626.

Clement, A.C., M.A. Cane and R. Seager, 2001: An orbitally driven tropical source for abrupt climate change. *J. Climate*, **14**, 11, 2,369-2,375.

Clement, A., R. Seager and Mark A. Cane, 2000: Suppression of El Niño during the mid-holocene by changes in the earth's orbit, *Paleoceanogr.*, **15**, 731-737.

Cobb, K.M., C.D. Charles, R.L. Edwards, H. Cheng, and M. Kastner, 2003: El Niño-Southern Oscillation and tropical Pacific climate during the last millennium, *Nature* **424**, 271-276.

Collins, M., 2000: Understanding Uncertainties in the response of ENSO to Greenhouse Warming. *Geophys. Res. Letts*., **27**(21), 3509-3513.

Collins, M. and the CMIP Modelling Groups 2004: El Niño or La Niña –like climate change? *Geophys Res Lett.* Submitted.

Crowley, T.J., 2000: Causes of Climate Change Over the Past 1000 years, *Science,* **289**, 270-277.

D'Arrigo, R., R. Villalba, and G. Wiles, Tree-ring estimates of Pacific decadal climate variability, *Climate Dynamics*, *18*, 219-224, 2001.

Doherty, R. and M. Hulme, 2002: The relationship between the SOI and the extended tropical precipitation in simulations of future climate change. *Geophys. Res. Letts*., **29**(10), 1475, 10.1029/2001GLO14601.

Davis, M., 2001: *Late Victorian Holocausts: El Nino Famines and the Making of the Third World.* Verso Press, London/New York 465 pp.

Deser, C., A.S. Phillips and J.W. Hurrell, 2004: Pacific Interdecadal Climate Variability, Linkages between the Tropics and North Pacific during boreal winter since 1900. *J. Climate,* submitted.

Evans, M.N., A. Kaplan and M.A. Cane, 2000: Intercomparison of coral oxygen isotope data and historical SST: Potential for coral-based SST field reconstructions. *Paleoceanogr*. **15**, 551-563.

Evans, M. N., M. A. Cane, D. P. Schrag, A. Kaplan, B. K. Linsley, R. Villalba, G. M. Wellington, 2001: Support for tropically-driven Pacific decadal variability based on paleoproxy evidence, *Geophysical Research Letters*, **28** (19), 3689-3692.

Evans, M. N., A. Kaplan, and M.A. Cane, 2002: Pacific sea surface temperature field reconstruction from coral $d^{18}O$ data using reduced space objective analysis, *Paleoceanography***,** **17** (1), 10.1029/2000PA000590.

Federov, A.V. and S.G. Philander, 2000: Is El Niño Changing? *Science*, **288**, 1,997-2,002.

Fedorov, A.V. and Philander, S.G.H. 2001: A stability analysis of tropical Ocean-Atmosphere Interactions (Bridging Measurements of, and Theory for El Niño). *J.Climate,* **14**, 3086-3101.

Garreaud, R.D. and D.S. Battisti, 1999: Interannual and interdecadal variability of the tropospheric circulation in the Southern Hemisphere. *J. Climate***,** **12**, 2113-2123.

Gedalov, Z., and D.J. Smith, Interdecadal climate variability and regime-scale shifts in Pacific North America, *Geophysical Research Letters*, **28** (8), 1515-1518, 2001.

Gershunov, A. and T.P.Barnett. 1998: Interdecadal modulation of ENSO teleconnections *Bull Amer. Met. Soc,.* **79,** 2715-2725.

Goddard, L., 2004: El Niño: Catastrophe or opportunity? *J. Climate*, submitted.

Goddard, L., S.J. Mason, S.E. Zebiak, C.F. Ropelewski, R. Basher and M.A. Cane, 2001: Current approaches to seasonal to interannual climate predictions. *International J. of Climatology*, **21**, 1,111-1,152.

Hughen, K.A., D.P. Schrag, S.B. Jacobsen, and W. Hantoro, 1999: El Niño During the Last Interglacial Period Recorded by a Fossil Coral from Indonesia, *Geophys. Res. Lett***.** **26**, 3129-3132.

Jones, P.D., T.J. Osborn, and K.R. Briffa, 2001: The Evolution of Climate over the Last Millenium *, Science*, **292**, 662-667.

Kaplan, A., M., A. Cane, Y. Kushnir, A. C. Clement, B. Blumenthal, and B. Rajagopalan, 1998: Analyses of global sea surface temperature, 1856 - 1991, *J. Geophys. Res.,* **103**, 18,567-18,589.

Koutavas, A., J. Lynch-Stieglitz, T. M. Marchitto, and J. P. Sachs, 2002: El Nino-like patter in ice age tropical Pacific sea surface temperature, *Science*, **297**, 226-230.

Kumar, K., B. Rajagopalan and M.A. Cane, 1999: On the weakening relationship between the Indian Monsoon and ENSO. *Science*, **284**, 2,156-2,159.

Latif, M., R. Kleeman and C. Eckert, 1997: Greenhouse warming, decadal variability, or El Niño? AN attempt to understand the anomalous 1990s. *J. Climate.,* **11,** 2325-1339.

Mann, M.E., R.S. Bradley and M.K. Hughes, 2000: Long-Term Variability in the El Niño/Southern Oscillation and Assocciated Teleconnections, in *"El Niño and the Southern Oscillation*. Multiscale Variability and Global and Regional Impacts. Eds. by Henry F. Diaz and Vera Markgraf, Cmbridge University Press.

Mann, M.E. 2002, The Value of Multiple Proxies, *Science*, **297**, 1481-1482.

Mann, M.E., M.A. Cane, S.E. Zebiak and A. Clement, 2004: Volcanic and solar forcing of El Niño over the past 100 years. *J. Climate*, accepted.

Mantua, N.J., S.R. Hare, Y. Zhang, J.M. Wallace, and R.C. Francis, 1997: A Pacific interdecadal oscillation with impacts on salmon production, *Bulletin of the American Meteorological Society*, **78**, 1069-10079.

Moy, C. M., G. O. Seltzer, D. T. Rodbell, and D. M. Anderson, 2002: Variability of El Niño/Southern Oscillation activity at millennial timescales during the Holocene epoch, *Nature*, **420**, 162-165.

Otto-Bleisner, B.L., E.C. Brady, S-I Shin, Z. Liu, and C. Shields, 2003: Modeling El Niño and its tropical teleconnections during the last glacial-interglacial cycle, *Geophys. Res. Lett.,* **30**, 2198, doi: 10.1029/2003GL018553.

Power, S., T. Casey, C. Folland, A. Colman, and V. Mehta, 1999: Inter-decadal modulation of the impact of ENSO on Australia, *Climate Dynamics*, **15** (5), 319-324.

Rajagopalan, B., U. Lall, and M.A. Cane, 1997: Anomalous ENSO Occurrences: An Alternate View, *J. Climate.*, **10**, 3251-2357.

Rodbell, D., G. Seltzer, D. Anderson, M. Abbott, D. Enfield, and J. Newman, 1999. An 15,000 year record of El Niño-driven alluviation in southwestern Ecuador. *Science*, **283**, 516-520.

Sandweiss, D., J. Richardson, E. Reitz, H. Rollins, 1996. Geoarchaeological evidence from Peru for a 5000 year B.P. onset of El Niño. *Science*, **273**, 1,531-1,533.

Timmermann, A., J. Oberhuber, A. Bacher, M. Esch, M. Latif, E. Roeckner, 1999. Increased El Niño frequency in a climate model forced by future greenhouse gas warming, *Nature,* **398**, 694-696.

Trenberth, K.E., and T.J. Hoar, 1997. El Niño and climate change, *Geophys. Res. Lett.*, 24, 3057-3060.

Tudhope, A.W., C.P. Cilcott, M.T. McCulloch, E.R. Cook, J. Chappell, R.M. Ellam, D.W. Lea, J.M. Lough and G.B. Shimmield, 2001. Variability in the El Niño-Southern Oscillation Through a Glacial-Interglacial Cycle. *Science*, **291**, 1511–1517.

Villalba, R., R.D. D'Arrigo, E.R. Cook, G.C. Jacoby, and G. Wiles, 2001. Decadal-scale climate variability along the extratropical western coast of the Americas: Evidence from tree-ring records, in *Interhemispheric Climate Linkages*, edited by V. Markgraf, pp. 155-172, Academic Press, San Diego.

Wunsch, C., 1999: The interpretation of short climate records, with comments on the North Atlantic and Southern Oscillations. *Bull. Amer. Met. Soc.,* **80,** 245-255.

Zebiak, S.E. and M.A. Cane, 1987: A model El Niño/Southern Oscillation, *Mon. Weather Rev,.* **115**, 2262-2278.

Zhang, Y., J.M. Wallace, and D.S. Battisti, 1997: ENSO-like interdecadal variability: 1900-93, *J.Climate,***10**, 1004-1020.

Figures

1. Measures of El Niño and of the Southern Oscillation, 1866-2003. The red curve is a commonly used index of El Niño, the sea surface temperature (SST) anomaly in the NINO3 region of the eastern equatorial Pacific (90°W-150°W, 5°S-5°N). The blue curve is the sea level pressure (SLP) at Darwin, Australia, an index of the atmospheric Southern Oscillation. The close relationship between the two indices is evident. (Departures in the earliest part of the record are more likely due to data quality problems than to real structural changes in ENSO.)

2. Schematics of Normal Conditions and El Niño Conditions in the equatorial Pacific Ocean and atmosphere to illustrate the Bjerknes feedback. In the "normal" state, the thermocline is near the surface in the east and temperatures there are cold. The easterly trades are strong. The stronger winds pull the thermocline up and increase upwelling; the stronger east-west sea surface temperature (SST) gradient creates a stronger east west sea level pressure (SLP) gradient (a more positive Southern Oscillation), that drives stronger winds. In the El Niño state, the winds relax, the thermocline deepens in the east and the temperatures there warm. The SST and SLP gradients decease, weakening the trade winds, and the warm state is reinforced.

3. The evolution of the ENSO cycle, illustrating the delayed oscillator mechanism and the Bjerknes feedback. The field indicates thermocline displacement and the arrow wind stress. See text for an explanation. The figures derive from an implementation of the model of Cane, Munnich, and Zebiak (1990). Briefly, a shallow water rectangular ocean on an equatorial beta plane is driven by a wind of the form $A\ exp(\mu\ y^2/2)$ over the middle 30% of the basin. The amplitude A depends on the thermocline depth at the eastern end of the equator, a proxy for the SST gradient. The model may be run at <http://ocp.ldeo.columbia.edu/enso/>

4. Paleo-ENSO variability from fossil corals. From Tudhope et al (2001). (A) Left hand side: Seasonal resolution (thin lines) and 2.25 year binomial filtered (thick lines) skeletal $\delta^{18}O$ records from fossil corals from the Huon Peninsula, with the record from modern coral DT91-7 shown for comparison. Right hand side: 2.5-7year (ENSO) bandpass filtered coral $\delta^{18}O$ timeseries. (B) Standard deviation of the 2.5-7 year (ENSO) bandpass filtered timeseries of all modern and fossil corals shown in (A). An asterisk after the coral label indicates that the timeseries is < 30 years long. The horizontal dashed lines indicate maximum and minimum values of standard deviation for sliding 30-year increments in the modern coral records.

5. After Mann et al (2004). Comparison of the ensemble annual mean Niño3 response to the combined volcanic and solar radiative forcing over the interval AD 1000-1999. a) Response (red--anomaly in ^{o}C relative to AD 1000-1999 mean) to radiative forcing (blue) based on an ensemble of 100 realizations. b)

Comparison of model ensemble-mean Niño3 (gray--anomaly in ^{o}C relative to AD 1950-1980 reference period; 40 year smoothed values shown by thick maroon curve) with reconstructions of ENSO behavior from Palmyra coral oxygen isotopes (blue--the annual means of the published monthly isotope data are shown). The coral data are scaled so that the mean agrees with the model (see Mann et al (2004) for details). Warm-event (cold-event) conditions associated with negative (positive) isotopic departures. Thick dashed lines indicate averages of the scaled coral data for the three available time segments (blue) and the ensemble-mean averages from the model (red) for the corresponding time intervals. The associated inter-fourth quartile range for the model means (the interval within which the mean lies for 50% of the model realizations) is also shown. The ensemble mean is not at the center of this range, due to the skewed nature of the underlying distribution of the model Niño3 series. Also shown (green curve) is the 40 year smoothed model result based on the response to volcanic forcing only, with the mean shifted to match that of the coral segments.

6. (a) The trend in monthly mean SST anomalies from 1900 to 2000 in °C per century. Updated from Cane et al (1997) Regions that cool, such as the eastern equatorial Pacific, are significantly different from the mean global SST warming of 0.4°C per century. (b) Time series of: (top) the average SST anomaly in the WP region (120°E to 160°E; 5°N to 5°S); (middle) average SST anomaly in the NINO3.4 region (120°W to 170°W; 5°N to 5°S); (bottom) the difference WP-NINO3.4, a measure of the zonal SST gradient. The linear trends in the 3 time series (°C per century) are 0.41±0.06, -0.08±0.25, and 0.50±0.25, respectively.

7. (a) Un-weighted histogram of a measure of ENSO (called "ENSOness" in Collins et al (2004)) of the pattern of climate change in the CMIP 1%/year increase of greenhouse gas experiments. The histogram is normalized to give probability values. A bin size of 0.5 is used with bins centered on 0, +/-0.5, +/-1, etc. (b) Histogram of "ENSOness" weighted by the ENSO Simulation Index (ESI), a measure of the realism of the model control run ENSO cycle. Bin sizes etc. as in (a). (c) ENSOness measure against ESI for the CMIP models. Those models with the more realistic ENSO cycle tend to have a smaller amplitude trend towards either El Niño-like or La Niña-like change. From Collins et al (2004).

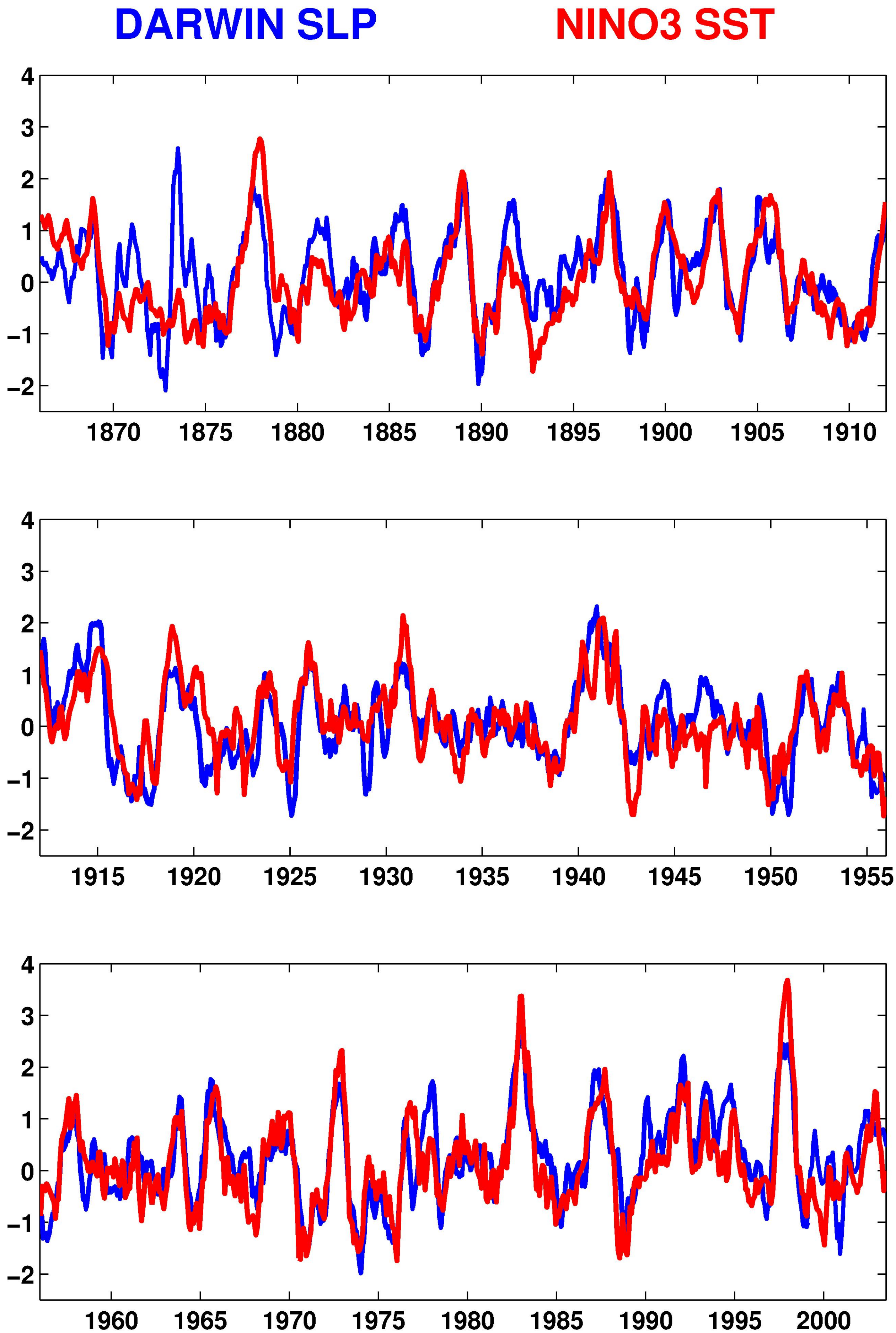
DARWIN SLP
NINO3 SST
4
3
2
1
0
−1
−2
1870
1875
1880
1885
1890
1895
1900
1905
1910
1915
1920
1925
1930
1935
1940
1945
1950
1955
1960
1965
1970
1975
1980
1985
1990
1995
2000

Normal Conditions

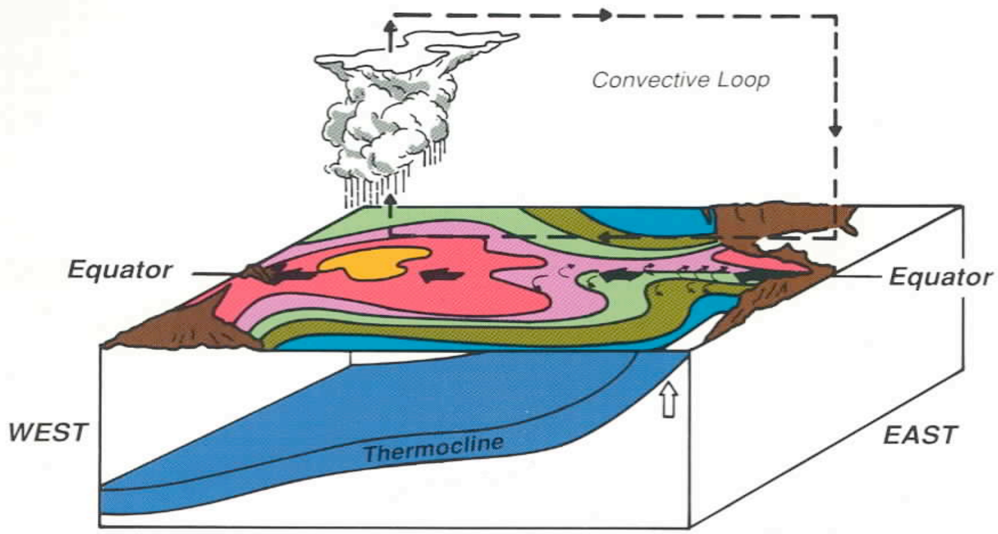

El Niño Conditions

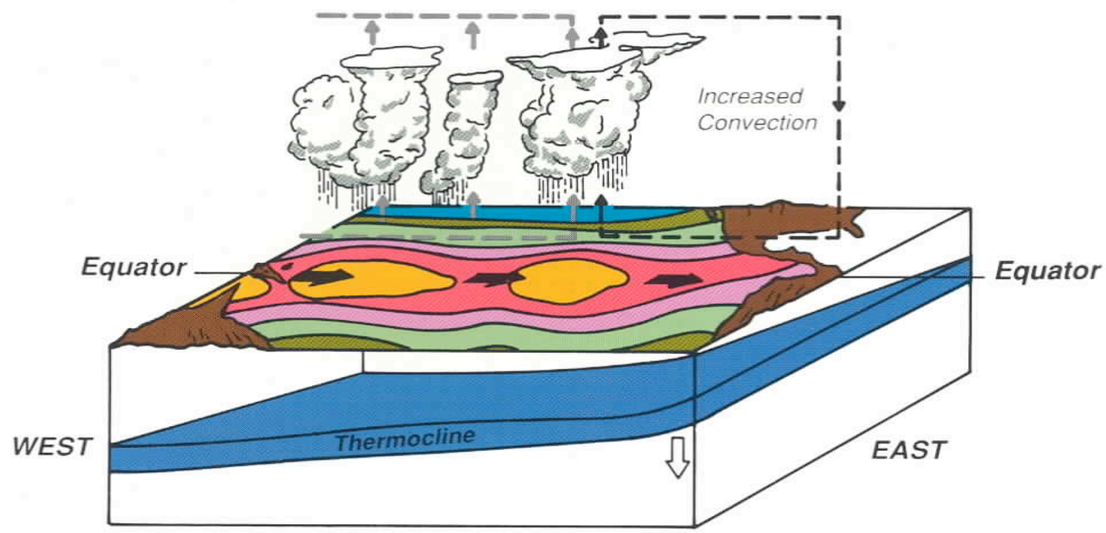

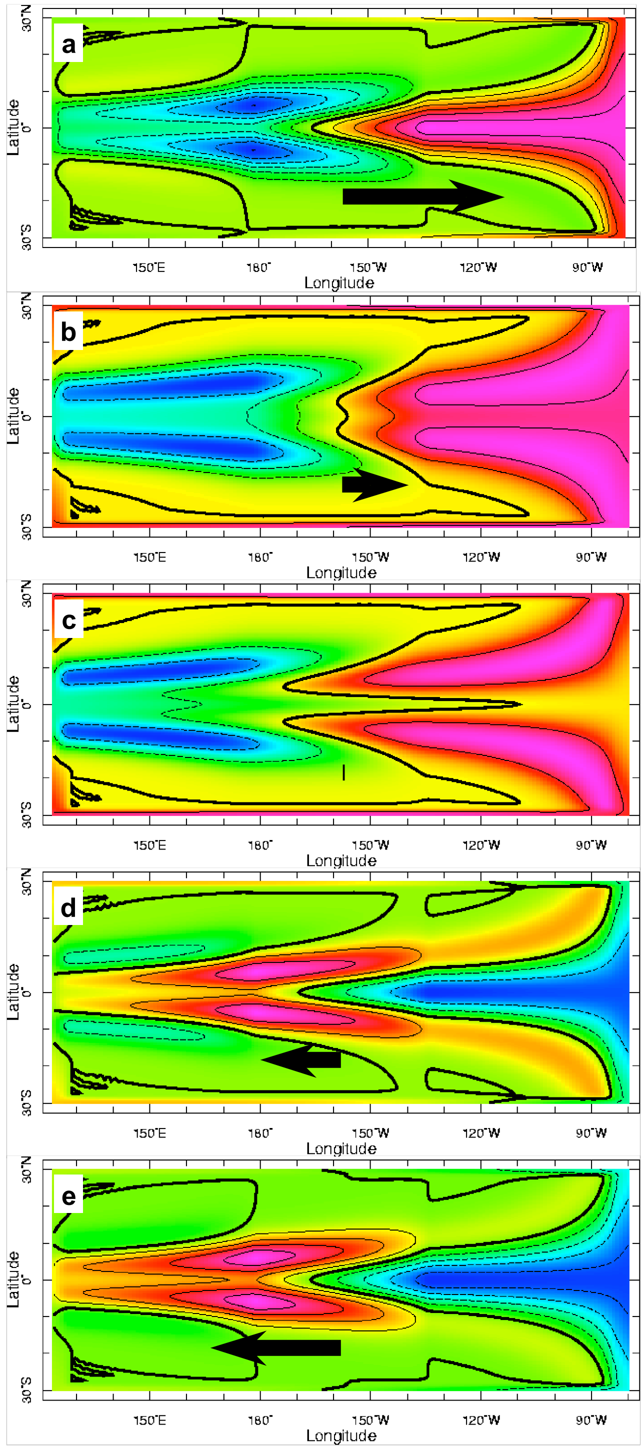
a
b
c
d
e
Latitude
30°N
0°
30°S
150°E
180°
150°W
120°W
90°W
Longitude

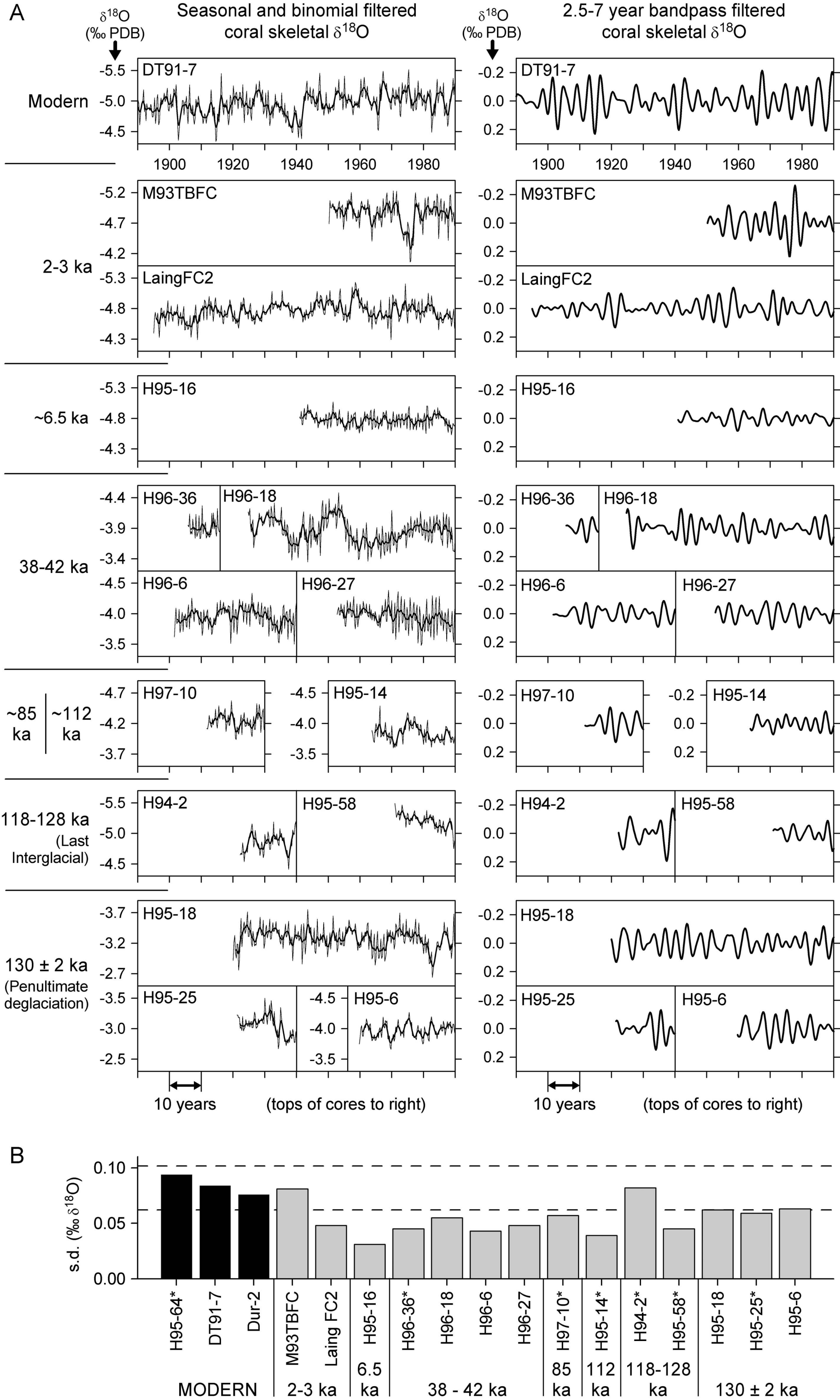

A
Seasonal and binomial filtered coral skeletal δ18O
2.5-7 year bandpass filtered coral skeletal δ18O
δ18O (‰ PDB)
Modern
DT91-7
2-3 ka
M93TBFC
LaingFC2
~6.5 ka
H95-16
38-42 ka
H96-36
H96-18
H96-6
H96-27
~85 ka
~112 ka
H97-10
H95-14
118-128 ka (Last Interglacial)
H94-2
H95-58
130 ± 2 ka (Penultimate deglaciation)
H95-18
H95-25
H95-6
1900
1920
1940
1960
1980
10 years
(tops of cores to right)
B
s.d. (‰ δ18O)
0.10
0.05
0.00
H95-64*
DT91-7
Dur-2
M93TBFC
Laing FC2
H95-16
H96-36*
H96-18
H96-6
H96-27
H97-10*
H95-14*
H94-2*
H95-58*
H95-18
H95-25*
H95-6
MODERN
2-3 ka
6.5 ka
38 - 42 ka
85 ka
112 ka
118-128 ka
130 ± 2 ka

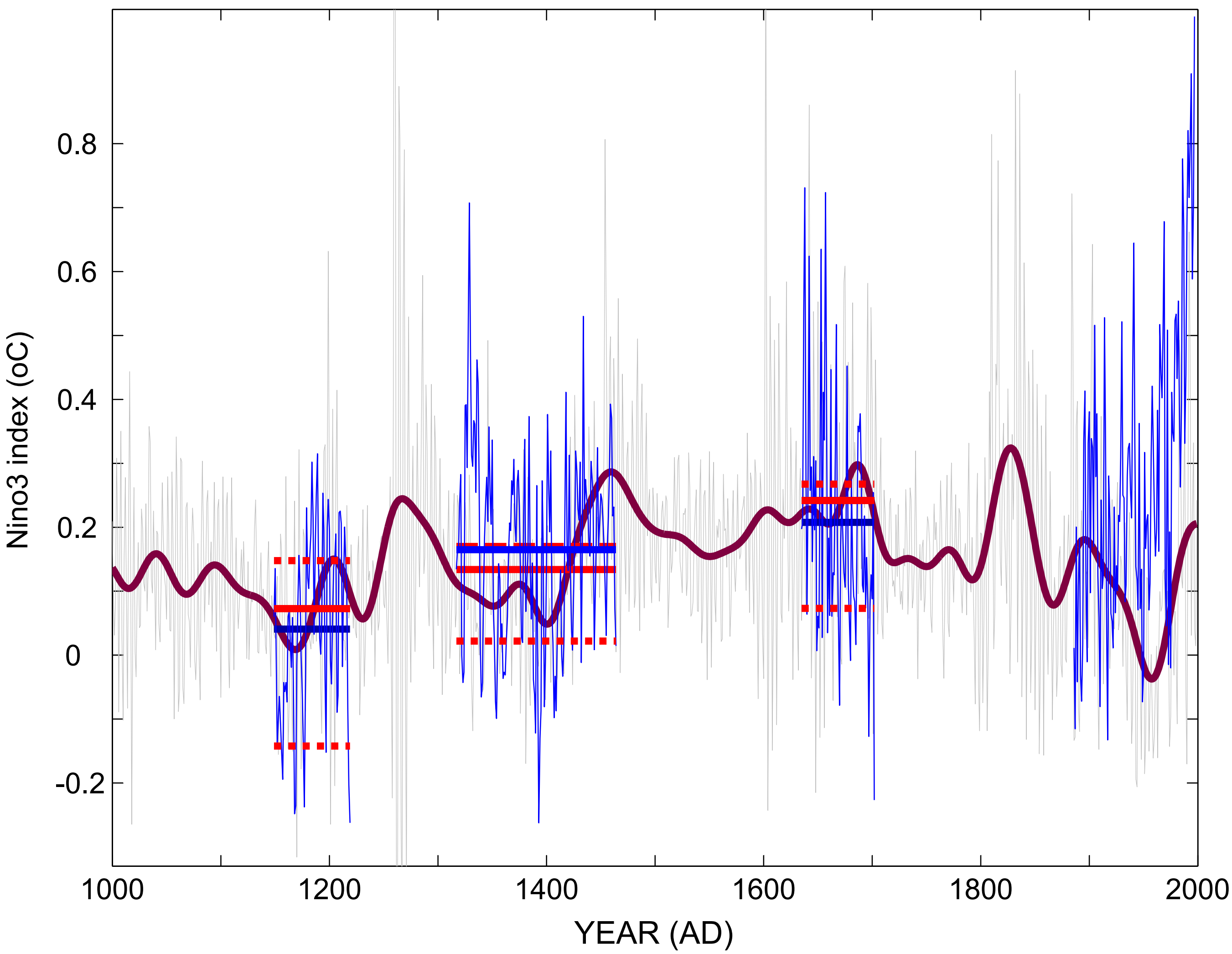
0.8
0.6
0.4
0.2
0
-0.2
Nino3 index (oC)
1000
1200
1400
1600
1800
2000
YEAR (AD)

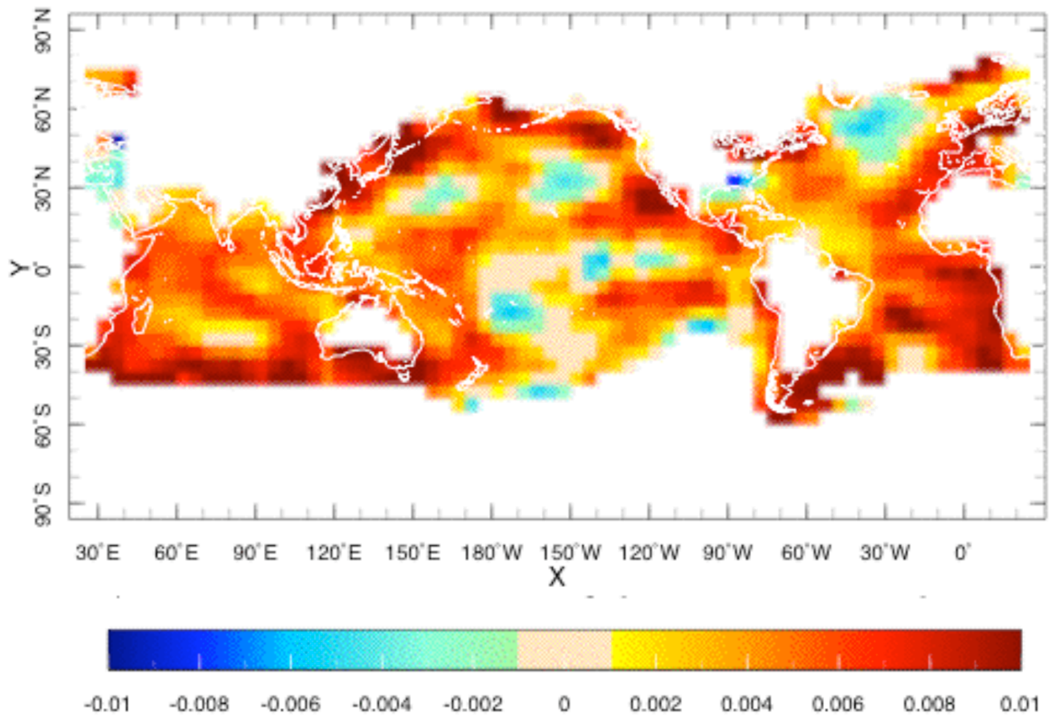
90°N
60°N
30°N
0°
30°S
60°S
90°S
Y
30°E
60°E
90°E
120°E
150°E
180°W
150°W
120°W
90°W
60°W
30°W
0°
X
-0.01
-0.008
-0.006
-0.004
-0.002
0
0.002
0.004
0.006
0.008
0.01

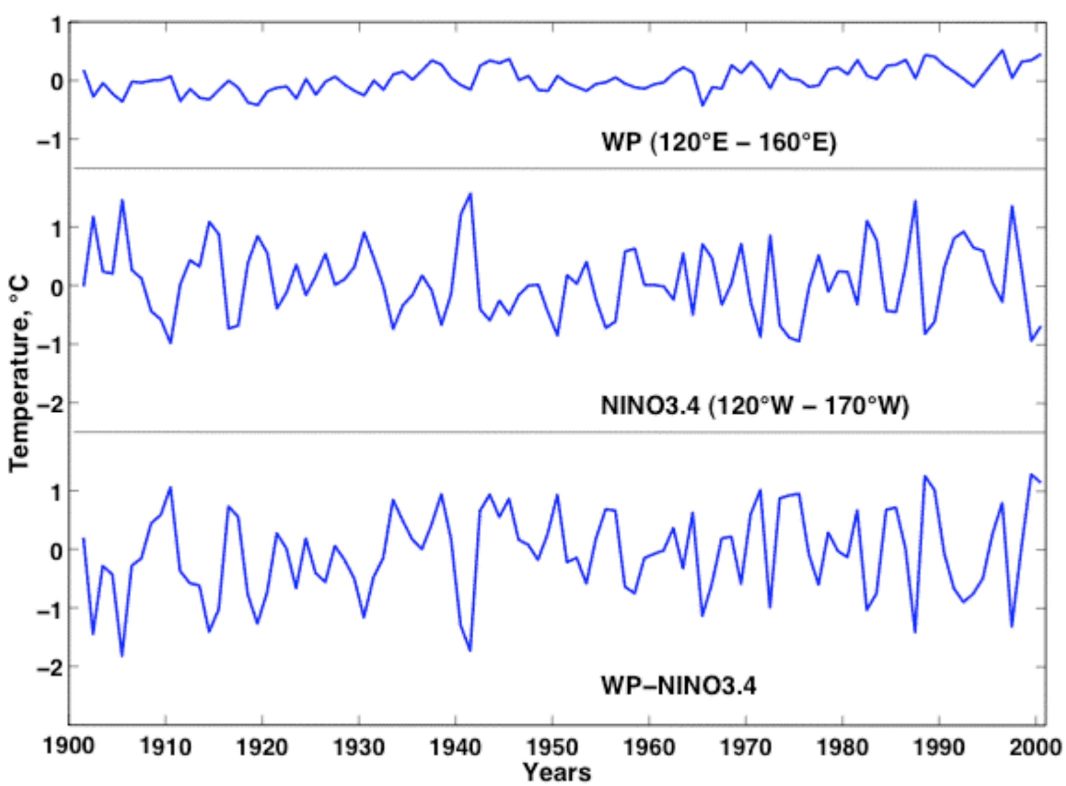
WP (120°E – 160°E)
NINO3.4 (120°W – 170°W)
WP–NINO3.4
Temperature, °C
1
0
−1
−2
1900
1910
1920
1930
1940
1950
1960
1970
1980
1990
2000
Years

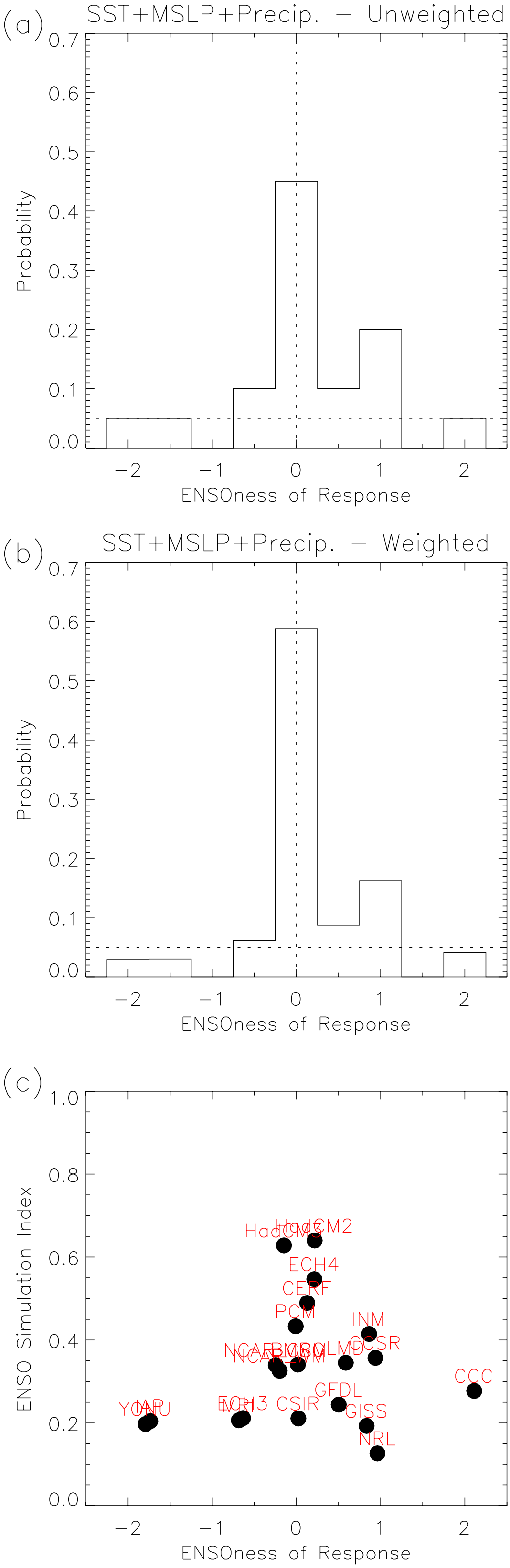
(a)
SST+MSLP+Precip. – Unweighted
Probability
ENSOness of Response
(b)
SST+MSLP+Precip. – Weighted
Probability
ENSOness of Response
(c)
ENSO Simulation Index
ENSOness of Response
HadCM2
HadCM3
ECH4
CERF
PCM
INM
CCSR
NCAR-WM
BMRC
LMD
CCC
GFDL
CSIR
GISS
NRL
YONU
IAP
MRI
ECH3